archives
of thermodynamics
Vol. **43**(2022), No. 4, 85–108
DOI: 10.24425/ather.2022.144407

Design of thermoelectric radiant cooling – photovoltaic panels system in the building

ISRAA ALI ABDULGHAFOR
MOHANNAD JABBAR MNATI*

Middle Technical University, Institute of Technology Baghdad,
Al-Za'franiya, 10074, Baghdad, Iraq

Abstract In this study, a theoretical model is presented to investigate the performance of a thermoelectric (TE) radiant cooling system combined with photovoltaic (PV) modules as a power supply in a building with an ambient temperature reaching more than 45°C. The combined system TE/PV performance is studied under different solar radiation by using the hourly analysis program and photovoltaic system software. The thermal and electric characteristics of TE are theoretically investigated under various supplied voltages using the multi-paradigm programming language and numerical computing environment. Also, a theoretical analysis of heat transfer between the TE radiant cooling system and an occupied zone from the side, and the other side between the TE radiant cooling system and duct zone is presented. The maximum power consumption by TE panels and building cooling load of 130 kW is predicted for May and June. The 145 units of PV panels could provide about 50% of the power required by TE panels. The thermal and electric characteristics of TE panels results show the minimum cold surface temperature of 15°C at a supplied voltage between 6 V and 7 V, and the maximum hot surface temperature of 62°C at a supplied voltage of 16 V. The surface temperature difference between supplied current and supplied power increases as supplied voltage increases. At a higher supplied voltage of 16 V, the maximum surface temperature difference between supplied current, and supplied power of 150°C, 3.2 A, and 48 W, respectively. The cooling capacity increases as supplied voltage increases, at a surface temperature difference of –10°C and supplied voltage of 16 V, the maximum cooling capacity is founded at about 60 W. As supplied voltage

*Corresponding Author. Email: mohannad.mnati@mtu.edu.iq

decreases the coefficient of performance increases. The maximum coefficient of performance is about 5 at the surface temperature difference of –10°C and supplied voltage of 8 V.

Keywords: Thermoelectric panels; Cooling capacity; Numerical calculations; PV system

Nomenclature

A	–	area, m^2
COP	–	coefficient of performance
g	–	gravitational acceleration, m/s^2
Gr	–	Grashof number
h	–	heat convection coefficient, $W/(m^2K)$
I	–	current, A
K	–	thermal conductance, W/K
k	–	thermal conductivity, W/(m·K)
L_c	–	characteristic length, m
MRT	–	mean radiant temperature, °C
Nu	–	Nusselt number
NTE,c	–	number of thermoelectric cooling panels
P	–	electrical power consumption, W
Pr	–	Prandtl number
Q	–	heat transfer rate, W
q	–	heat flux, W/m^2
Ra	–	Rayleigh number
Re	–	Reynolds number
T	–	temperature, °C
T_c	–	temperature of a cold surface, °C
T_h	–	temperature of a hot surface, °C
τ	–	thickness, m
U	–	overall heat transfer coefficient, $W/(m^2K)$
υ	–	kinematic viscosity, m^2/s
v	–	supplied voltage, V

Greek symbols

α	–	seebeck coefficient of the thermocouple, V/K
ε	–	emissivity
σ	–	Stefan-Boltzmann constant, $W/(m^2K^4)$
ρ	–	density, kg/m^3
β	–	coefficient of cubical expansion, 1/°C
μ	–	viscosity, kg/(m·s)

Subscripts

a	–	air
Al	–	aluminum
b	–	base
c	–	cold
cond	–	conduction

d – duct
d-ins – between the duct and thermal insulation
h – hot
ins – thermal insulation
max – maximum
p – plate
p_{TE} – thermoelectric panel
rad – radiation

Abbreviation

HAP – Hourly Analysis Program
MTU – Middle Technical University
PV – photovoltaic
TE – thermoelectric

1 Introduction

In hot and dry weather, temperature control in houses, hospitals, laboratories, and classrooms in schools and universities is considered a vital requirement [1]. But the environment is affected by the lifestyle. The earth's climate is largely affected by greenhouse gas and the stability of the current climate is jeopardized by increasing greenhouse gas emissions produced by people's activities [2]. The carbon dioxide (CO_2) results from burning fossil fuels, the primary gas that causes global warming [3], and the rising energy demand have caused a significant increase in the emissions of CO_2 to the atmosphere [4]. The cooling and heating refrigeration systems have an essential role in this increase [5]. In the last decades, the refrigerant's effect on the environment has become the primary issue. Due to large leaks in the cooling system, these refrigerants are responsible for ozone layer depletion and rising greenhouse gas impact [6]. Also, the electric consumption by the refrigeration cooling and heating systems indirectly participates to increase the emission of CO_2 [7]. Therefore, designing friendly cooling and heating systems integrated with renewable electricity sources is of great significance to saving energy and reducing environmental problems. The thermoelectric (TE) panels have been utilized in many applications such as heat recovery solar still, solar panels, and cooling and heating systems [8].

Due to the impact of Peltier, TE panels are used in cooling and heating system which offer some attractive features such as no requirement for major mobile parts or refrigeration, quiet process, excellent controllability, little maintenance, and stability. TE panels consist of two elements of a doped semiconductor, n-type and p-type, which are linked electrically as

a series and thermally as a parallel [9]. A different arrangement is possible for installing TE panels in the building so they can be installed in walls, windows, and ceiling. A few past studies have focused on ceiling TE panels. The radiant cooling and heating panels are provided to the building spaces by using TE panels. The mechanism of the TE radiant system is essentially by forming a cold/hot radiating surface by decreasing and increasing the temperature of the ceiling. The exchange of heat between the radiating surface and the human body occurs by radiation, so the radiant ceiling panels supply thermal comfort conditions for the occupant's zone [10].

In recent years, thermoelectric cooling and heating systems with photovoltaics have been studied in various applications. Xu *et al.* [11] investigated the coefficient of performance for the thermoelectric window integrated with the photovoltaic (PV) panels in the heating application. The results showed that the coefficient of performance (COP) of this system was 2.5. A solar-driven thermoelectric system for cooling was studied by Cheng *et al.* [12]. The waste heat of the photovoltaic and the hot side of the thermoelectric panels was used to produce hot water, at the same time, the indoor air cools by the cold side of the thermoelectric. Daghigh and Khaledian studied the coefficient of performance of the thermoelectric cooling and heating system integrated with the photovoltaic panel at an ambient temperature not exceeding 40°C [13]. The results appeared that when the voltage was 12 V, the coefficient of performance was 1. A thermoelectric fixed air duct system integrated with a photovoltaic wall to cool space has been analyzed by Irshad *et al.* [14]. The results showed that by increasing the input current from 2 A to 6 A, the coefficient of performance of the system enhancement by 71%, and the cooling power rose from 101.34 W to 517.24 W. As mentioned in past studies, the TE panel cooling radiant was never used at high ambient temperatures. In the summer season, Baghdad city suffers from many environmental problems such as a high ambient temperature which may reach 50°C, a high emission rate of CO_2 in the air, and high power consumption. Under the high ambient temperature, the cooling device performance decreases sharply with more electric power consumption and a rise in the emission rate of CO_2. So, the purpose of this study is to present a design for an efficient cooling system working in a high ambient temperature with minimal consumption of electrical power to decrease CO_2 emission by electric power plants and be environmentally friendly at Middle Technical University (MTU). Also, in this study, the performance of the designed system which consists of PV and TE panels is analyzed under different conditions.

2 System structure description

The proposed configuration of the thermoelectric radiant cooling-photovoltaic system installed in a building ceiling is shown in Fig. 1. It consists of PV panels, a battery, a controller of charge, thermoelectric panels, insulation, and an aluminum plate. The PV panels are utilized to produce the electricity required by TE panels. The PV panels are oriented in the south direction with a tilt angle of 30° to maximize the solar irradiance gain. They are connected to the thermoelectric panels that are attached from their cold surface to an aluminum plate that serves as a radiant cooling ceiling in the hot season as shown in Fig. 1, The thermoelectric panels cool the aluminum plate which absorbs the heat from the occupied zone by convection and radiation heat transfer. On the other hand, the heat generated by the hot surface of the thermoelectric panels is dissipated by utilizing outdoor air. To reduce unfavourable heat transfer to the air, the air surface of the thermoelectric panel should be insulated.

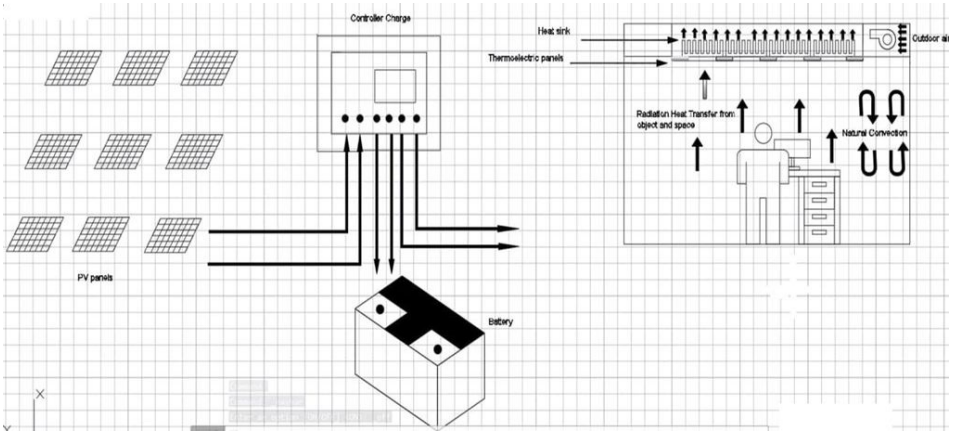

Figure 1: The proposal configuration of the thermoelectric radiant cooling-photovoltaic system.

3 System models

The mathematical models are produced *via* sub-models. The sub-models are produced depending on the system structure, which are PV panels, thermoelectric panels, and building energy. In this section, the main models are presented.

3.1 The photovoltaic model

In this study, the commercial PVsyst software package [15] is used to design a photovoltaic system. The selected PV system that has been chosen consists of 145 units of PV panels connected in series. The PV panel type selection is the most essential step in the PV system design. The PV panels type of monocrystalline technology is chosen due to its highest efficiency compared to other technologies. PV panel's rate power and total productions are 450 kW and 65 kW, respectively.

3.2 Thermoelectric radiant cooling system model

3.2.1 Thermal and electrical characteristics of thermoelectric panels

The TE panel's operating manner change with supplied input voltage so that for optimum performance of TE panels and restriction of the required input voltage, in this study, the thermal and electric characteristics of TE panels are studied theoretically under different available input voltage by using clean code in MatLab computing environment [16]. The clean code has been written by using the required function and boundary conditions to solve the equations, which determine the thermal and electric characteristics. The thermoelectric surface temperature with different voltage values must be known for cooling applications. The relationship between the supplied voltage (v) and temperature of the cooled surface (T_c), and temperature of the hot surface (T_h), can be expressed as follows [17]:

$$T_c = 0.009v^3 + 0.3194v^2 - 4.842v + 30.3030, \tag{1}$$

$$T_h = 0.0098v^3 - 0.0762v^2 + 0.7684v + 28.3961. \tag{2}$$

The temperature difference between the cold and hot surfaces (ΔT_{h-c}) is required in the cooling application. It can be calculated from the equation

$$\Delta T_{h-c} = 0.0073v^3 - 0.3575v^2 + 5.3430v - 1.3252. \tag{3}$$

To analyze the power consumption and thermoelectric internal resistance, the relationship between voltage and current must be known. In this study, the different voltages are considered since the voltage will be provided as the primary source of supply in cooling applications. The relationship between the voltage and current (I_{Supplied}) can be described by

$$I_{\text{Supplied}} = 0.1943v + 0.0219. \tag{4}$$

Power consumption (P_{Supplied}) for varying input voltage can be expressed as follows [18]:

$$P_{\text{Supplied}} = -0.0030v^3 + 0.2491v^2 - 0.2393v. \tag{5}$$

3.2.2 Heat transfer analysis of thermoelectric radiant cooling system

The steady-state heat flow from room air to outdoor air is shown in Fig. 2. The heat transfer from room air to outdoor air occurs through three modes.

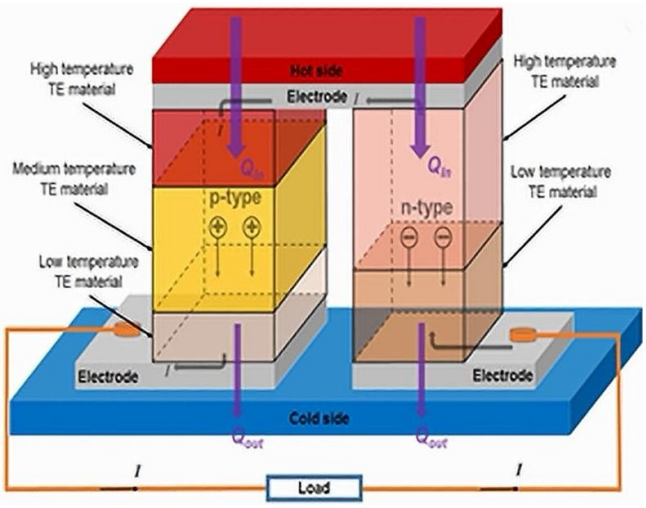

(a)

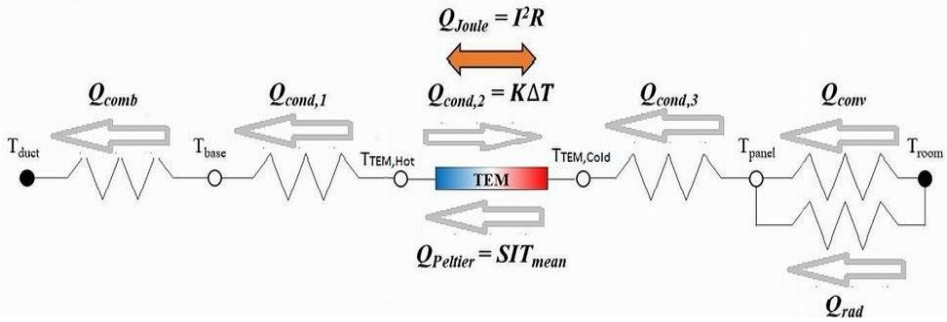

(b)

Figure 2: (a) Thermoelectric components. (b) Thermal resistance.

The heat is transferred by convection and radiation from room air to the surface of the aluminum plate. Then, the heat is conducted from the aluminum plate to the surfaces of thermoelectric radiant panels and the base plate of the heat sink, respectively, and the heat is transferred from the base plate of the heat sink to outdoor air by convection. For determining the convection heat transfer rate between an aluminum plate and room air, the heat transfer coefficient between an aluminum plate surface and room air (h_{a-p}) is calculated from

$$h_{a-p} = \frac{k_a \mathrm{Nu}}{L_c}\,, \tag{6}$$

where k_a represents the air thermal conductivity. The characteristic length L_c is calculated relative to the aluminum plate area [19]. The Nusselt number is defined by

$$\mathrm{Nu} = 0.27\mathrm{Ra}^{1/4} \quad \text{for} \quad 10^5 < \mathrm{Ra} < 10^{11}. \tag{7}$$

Here the Rayleigh number is given as

$$\mathrm{Ra} = \mathrm{Gr}\,\mathrm{Pr}, \tag{8}$$

where Pr denotes the Prandtl number and Gr is the Grashof number given as

$$\mathrm{Gr} = \frac{g\beta(T_a - T_p)L_c^3}{v_a^2}\,, \tag{9}$$

where g is the gravitational acceleration, β is the coefficient of cubical expansion, T_a is the air temperature, T_p is an aluminum plate temperature, and v_a is the kinematic viscosity.

The radiation heat transfer coefficient (h_{rad}) and the rate of radiation heat transfer between room air and an aluminum plate (Q_{rad}) are calculated by using equations, respectively:

$$h_{\mathrm{rad}} = \varepsilon_p \sigma \left(T_{\mathrm{MRT}}^2 + T_p^2\right)\left(T_{\mathrm{MRT}} + T_p\right), \tag{10}$$

$$Q_{\mathrm{rad}} = h_{\mathrm{rad}} A_p \left(T_p - T_{\mathrm{MRT}}\right). \tag{11}$$

Parameter ε_p represents the aluminum plate emissivity, σ is the Stefan-Boltzmann constant, and A_p is the area of the aluminum plate. For the internal zone, the radiant panels are usually fixed and present a low asymmetry of radiations so that the mean radiant temperature T_{MRT} is supposed to equal the temperature of room air T_a [20].

The rate of heat conduction from the aluminum plate to the cold surface of the thermoelectric panel ($Q_{\text{cond},1}$) and heat conduction from the hot surface of the thermoelectric panel to the base heat sink plate ($Q_{\text{cond},3}$) can be calculated by using the following simple equations of conduction heat transfer, respectively:

$$Q_{\text{cond},1} = k_{\text{pTE}} \frac{A_{\text{pTE}}}{\tau_b} \left(T_h - T_b\right), \tag{12}$$

$$Q_{\text{cond},3} = k_p \frac{A_p}{\tau_p} \left(T_p - T_c\right). \tag{13}$$

In Eq. (12), k_{pTE}, A_{pTE}, τ_b, and T_b represent the thermoelectric thermal conductivity, an area of the thermoelectric panel, the base plate thickness, and base plate temperature, respectively. Similarly, in Eq. (13) k_p, A_p, τ_p represent the aluminum plate's thermal conductivity, the area of the aluminum plate, and its thickness, respectively.

The overall coefficient of heat transfer between an aluminum plate surface and the duct air (U_{p-d}) can be determined as

$$U_{p-d} = \left(\frac{\Delta\tau_p}{k_p} + \frac{\Delta\tau_{\text{ins}}}{k_{\text{ins}}} + \frac{1}{h_{\text{d-ins}}} \right)^{-1}. \tag{14}$$

It consists of the thermal resistances of an aluminum plate $\dfrac{\Delta\tau_p}{k_p}$, and thermal resistances insulation $\dfrac{\Delta\tau_{\text{ins}}}{k_{\text{ins}}}$, where $\Delta\tau_{\text{ins}}$ and k_{ins} denote the insulation thickness and insulation thermal conductivity, respectively. The coefficient of convection heat transfer between the air and the air in the duct and the surface of the insulation is computed from

$$h_{\text{d-ins}} = \frac{k_a \text{Nu}}{L_c}. \tag{15}$$

The Nusselt number is calculated according to the Prandtl number value [21]:

$$\text{Nu} = \begin{cases} 0.66\text{Re}^{1/2}\text{Pr}^{1/3} & \text{for } \text{Pr} > 0.6, \ \ \text{Re} < 5, \\ 0.037\text{Re}^{0.8}\text{Pr}^{1/3} & \text{for } 0.6 \leq \text{Pr} \leq 60.5 \times 10^5, \ \ 10^5 \leq \text{Re} \leq 10^7. \end{cases} \tag{16}$$

The Reynolds number is defined as

$$\text{Re} = \frac{\rho_a \upsilon_a L_c}{\mu_a}, \tag{17}$$

where ρ_a and μ_a represent the air density and viscosity, respectively. The impact of the boundary layer velocity is supposed to be negligible because of the low coefficient of heat convection between the outdoor air and the thermal insulation.

3.2.3 Cooling performance analysis of thermoelectric radiant cooling panels

In this study, the cooling performance analysis of the TE cooling radiant system is investigated under different supplied voltages of TE panels. The cooling capacity Q_c can be defined as the rate of heat absorption at the cold surface of a thermoelectric panel and can be determined by

$$Q_c = \alpha I T_c - 0.5 I^2_{\text{Supplied}} - K(T_h - T_c), \tag{18}$$

where α and K represent the Seebeck coefficient of the thermocouple and thermal conductance, respectively [22].

The coefficient of performance of the TE cooling radiant system can be expressed as

$$\text{COP} = \frac{Q_c}{P_{\text{Supplied}}}\,. \tag{19}$$

The required number of thermoelectric panels to provide the peak cooling load ($Q_{c,\max}$) of the building can be determined using the formula

$$N_{\text{TE},c} = \frac{Q_{c,\max}}{q_c}\,, \tag{20}$$

where q_c is the cooling load flux.

Table 1 presents the initial and boundary conditions which are used to calculate the thermal and electric characteristics, and the cooling performance of the TE panel. The surface temperature difference means the difference between hot surface and cold surface temperatures. In some cases of operation, the hot surface temperature less than that of cold surface temperature so that cause the negative difference.

The specifications of the proposed thermoelectric panel are shown in Table 2.

Table 1: Initial and boundary conditions for calculating cooling performance and COP for TE panels.

Initial surface temperature			25°C
Supplied voltage range			1–16 V
v (V)	T_h (°C)	T_c (°C)	$T_h - T_c$ (°C)
8	32	42	–10
8	32	37	–5
8	32	32	0
8	32	27	5
8	32	22	10
12	32	42	–10
12	32	37	–5
12	32	32	0
12	32	27	5
12	32	22	10
16	32	42	–10
16	32	37	–5
16	32	32	0
16	32	27	5
16	32	22	10

Table 2: Specifications of the proposed thermoelectric panel.

T_h	25°C
$Q_{c,\max}$	60 W
$\Delta T_{\max}$	70°C
$V_{\mathrm{TE},c,\max}$	16.2 V
$I_{\mathrm{TE},c,\max}$	5.3 A

3.3 Building energy model

The case study is the classrooms on the second floor of the Electronic Technical Department in Baghdad Technology Institute, located at 33.26°N latitude, 44.49°E longitudes, and 36 m altitude. Figure 3 shows the building and floor that have been selected for this work. The area of the floor is approximately 1072 m^2. The external walls are constructed from the outside to inside from cement plaster 2 cm, common brick 24 cm, cement plaster 2 cm, and just plaster 2 cm. The roof is constructed with 20 cm of concrete. Every day, except for weekends and the standard Iraq holiday, the building

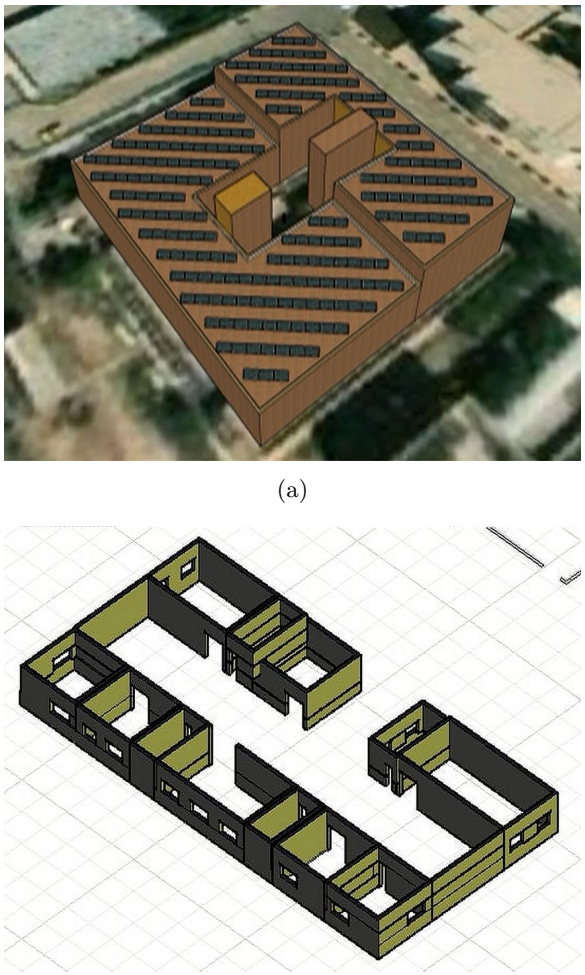

(a)

(b)

Figure 3: The building details: (a) building orientation, (b) second-floor details.

is occupied by 250 people least between 8 a.m. to 4 p.m. For the occupied hours, the set point of cooling is considered 25°C. By using the Hourly Analysis Program (HAP 4.6) for the design and analysis of commercial building heating, ventilation, and air conditioning (HVAC) systems [23], the building energy model is produced and the hourly cooling loads are computed for one year. The peak cooling loads are found as 130 kW for May and June. Table 3 presents the description of all doors and windows installed in the building and required by HAP.

Table 3: Windows and doors information.

Direction	Number	Frame kind	Dimensions (cm × cm)	Height from the ground (cm)
Windows				
North West	1	Iron	200 × 150	85
North West	2	Iron	148 × 230	85
North West	1	Iron	150 × 150	85
North East	2	Iron	200 × 150	85
North East	3	Iron	210 × 210	40
North East	4	Iron	250 × 152	85
North East	4	Iron	250 × 150	85
South East	3	Iron	200 × 146	85
Doors				
South West	4	Wood	200 × 85	–
South West	1	Iron	300 × 235	–
South West	2	Wood	200 × 170	–
North West	3	Wood	200 × 150	–
North West	2	Iron	200 × 85	–

4 Results and discussion

The results of thermal and electric characteristics, cooling performance analysis of thermoelectric panels, and the building energy modeling and the size of the system are listed and discussed in detail.

4.1 Thermal and electrical characteristics of thermoelectric panels

Figure 4a shows the relationship between the supplied voltage and cold and hot surface temperatures. From the results, it can be noticed that with the increases in supplied voltage from 1 V to 6 V, the cool surface temperature decreases, and the return begins to rise from 7 V to 16 V. Hot surface temperature increases gradually with the increases of supplied voltage from 1 V to 16 V. The minimum cool surface temperature of the thermoelectric panel of 14.915°C is obtained between 6 V and 7 V.

The relationship between the supplied voltage and the difference between the TE panel surfaces' temperatures can be seen in Fig. 4b. The

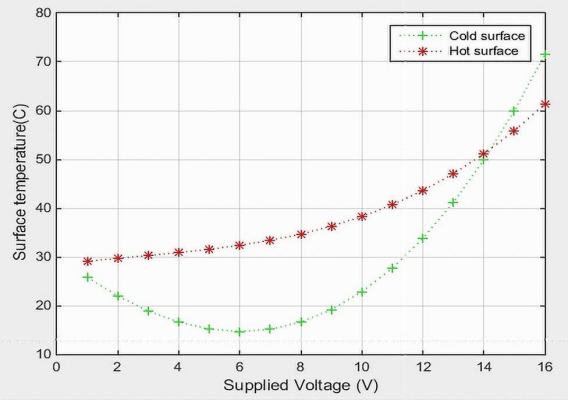

(a)

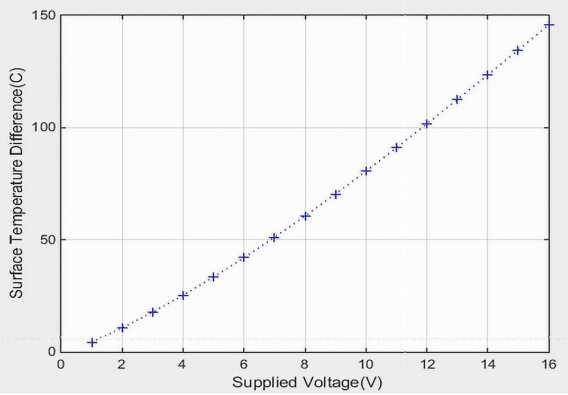

(b)

Figure 4: The relationship between supplied voltage and (a) cold and hot surfaces temperatures, (b) temperature difference between the cold and hot sides.

results show that the difference in temperature increases as supplied voltage increases and reaches the higher difference of 145.78°C for the high supplied voltage of 16 V. By comparing Figs. 4a and 4b it is clear that, although the gradient in temperature increases as supplied voltage increases, the cool surface temperature is not in its lowest value. This means that at the peak difference in temperature, the lowest cool surface temperature will not be obtained.

Changes in supplied current concerning changes in input voltage from 1 V to 16 V are demonstrated in Fig. 5a. The results refer to a linear relationship between the input voltage and input current. The input power

consumption by thermoelectric panels is given in Fig. 5b. It can be noticed that the power consumption increases as the input voltage increases. and the higher power of 48 W is obtained at 16 V.

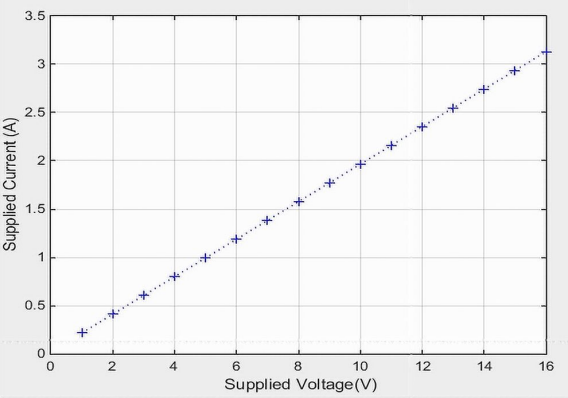

(a)

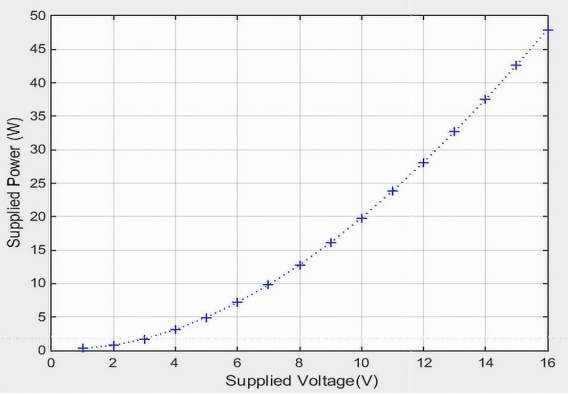

(b)

Figure 5: The relationship between supplied voltage and (a) input current, (b) input power.

4.2 Weather data, cooling load, and solar power

The building which is considered for simulation is in Al Za'franiya, Baghdad, Iraq. Al Za'franiya is located in the Baghdad southeast and has dry hot weather in the summer season. Typical weather information from HAP 4.6 library [23] is utilized as the reference for climate data for this simulation. Typical weather information from this library consists of 12 months

of hourly data, which represent the conditions of average climate in many years and therefore is considered a typical information group that can represent the climate information for a given location. The diagram of the building map as the three dimensional model constructed in computer-aided design software AutoCAD [24] is shown in Fig. 3. The solar flux data and outside dry bulb temperature for the hottest day in June and May are shown in Figs. 6 and 7, respectively. From Fig. 7 it can be noticed that at 3:00 p.m., the maximum dry and wet bulb temperatures are reached.

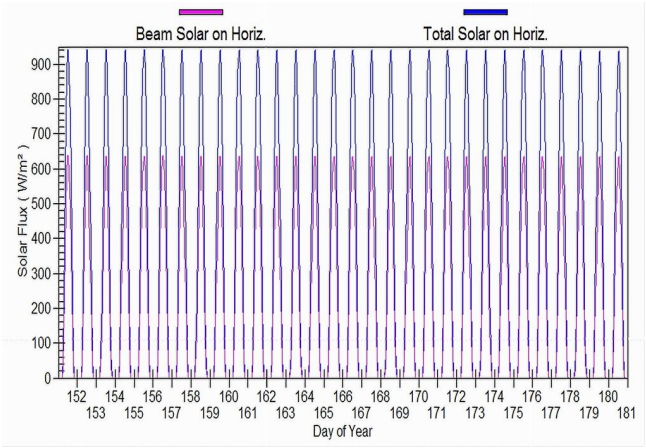

(a)

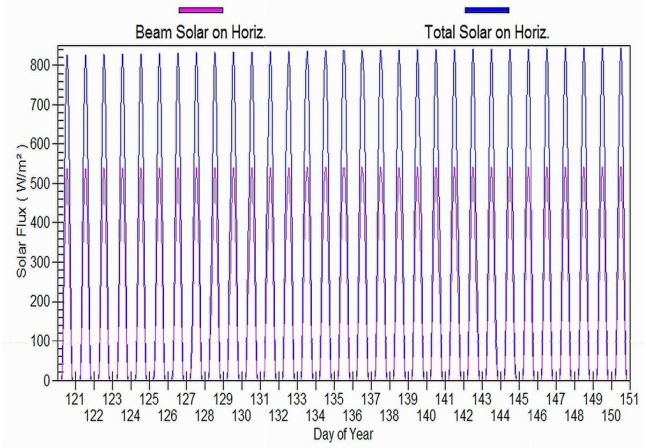

(b)

Figure 6: The solar flux: (a) June, (b) May.

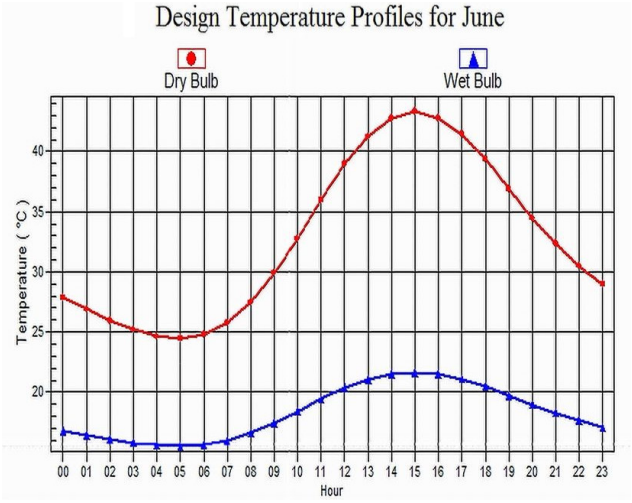

(a)

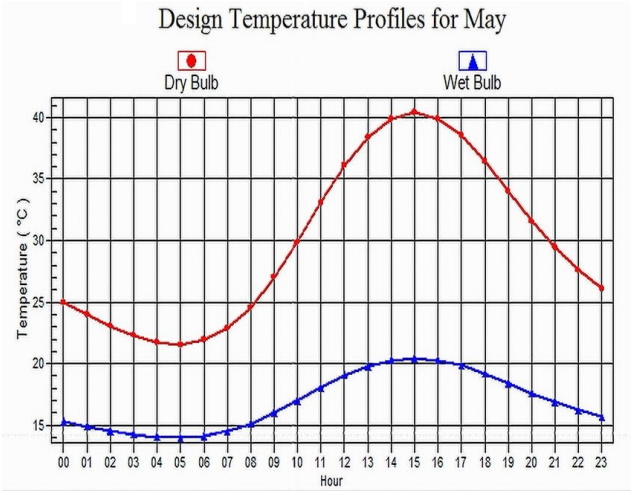

(b)

Figure 7: Dry and wet bulb temperature: (a) June, (b) May.

For June, the maximum dry bulb temperature exceeds 48°C, whereas for May it exceeds only 42°C.

The hourly cooling load for the hottest days, calculated by the HAP 4.6, is shown in Fig. 8. As mentioned above, the maximum dry temperature takes place at 3:00 p.m., hence the maximum hourly cooling load occurs

at 3:00 p.m., as depicted in Fig. 8. The peak hourly cooling load is found to occur in June and May between 7:00 a.m. and 3:00 p.m., and it reaches 130 kW and 128 kW, respectively. The total monthly cooling required for the building is determined and shown in Fig. 9. It is clear from Fig. 9, that the maximum monthly cooling load takes place in June and May, while the minimum monthly cooling load takes place in July and August since they are considered summer holidays.

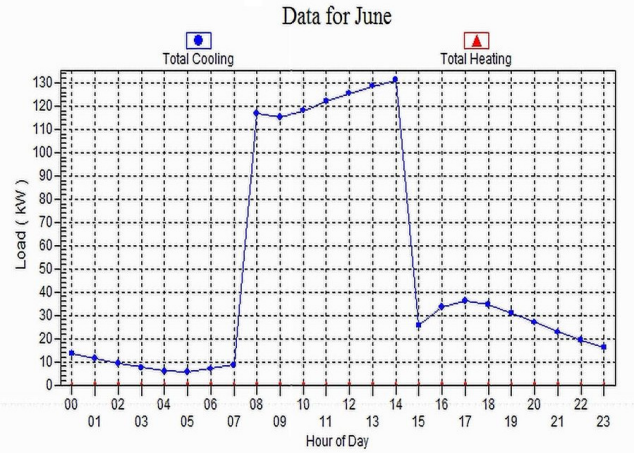

(a)

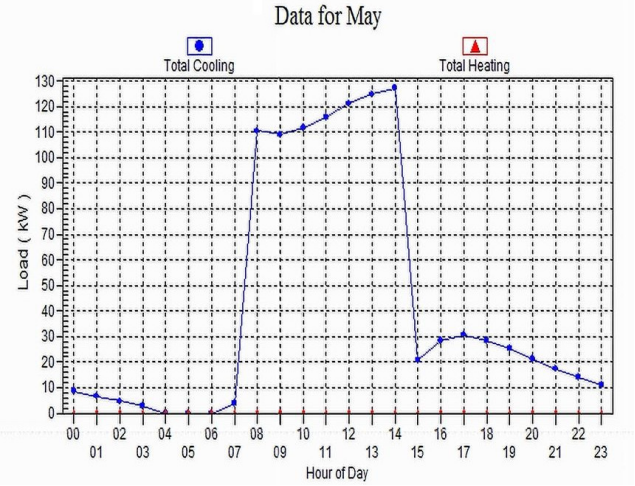

(b)

Figure 8: The cooling load: (a) June, and (b) May.

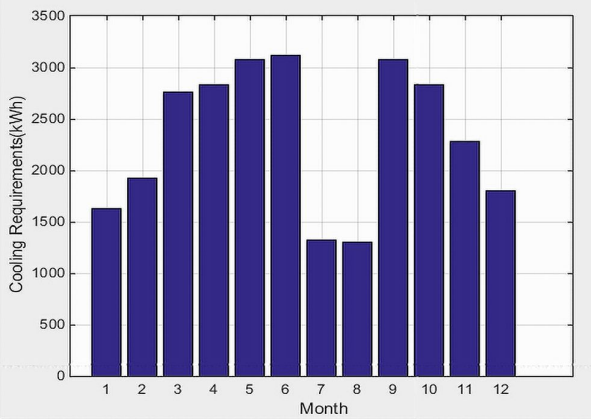

Figure 9: The monthly cooling load required.

4.3 Cooling performance analysis of thermoelectric radiant cooling system

For different voltages, the theoretical cooling capacity against the temperature difference between the cold and hot surfaces of the TE panel is presented in Fig. 10. With decreased temperature differences, the theoretical cooling capacity increases linearly. Also, the increase in supplied voltage leads to an increase in the theoretical cooling capacity. The ideal cooling capacity can be achieved at a voltage of 6 V and a temperature difference of –10°C.

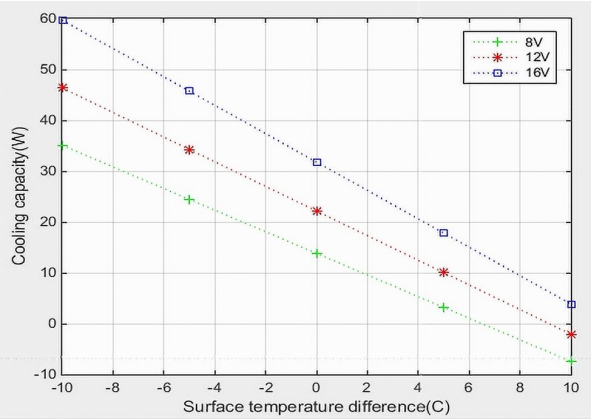

Figure 10: The relationship between cooling capacity and surface temperature difference for different voltages.

The Coefficient of performance of the TE panel against the temperature difference is shown in Fig. 11a. It can be concluded that as the temperature difference decreases the COP increases. Higher voltage leads to decreases in the COP against increasing temperature differences. For each voltage considered, the highest COP is predicted at a temperature difference of –10°C while the lowest COP at a temperature difference of 10°C. Figure 11b presents the variation of thermoelectric panel's number with COP for different voltages. It is clear that as COP increases the required number of TE panels increases due to a decrease in the cooling capacity with increas-

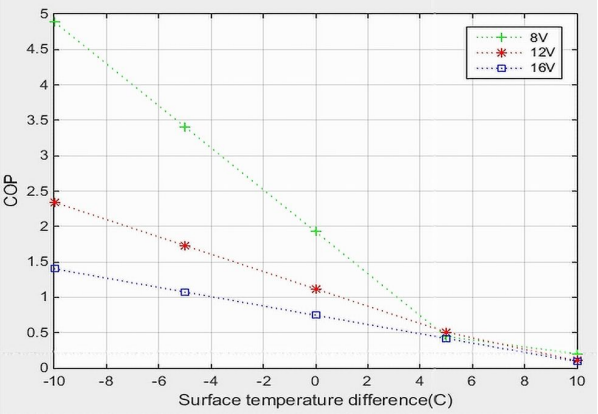

(a)

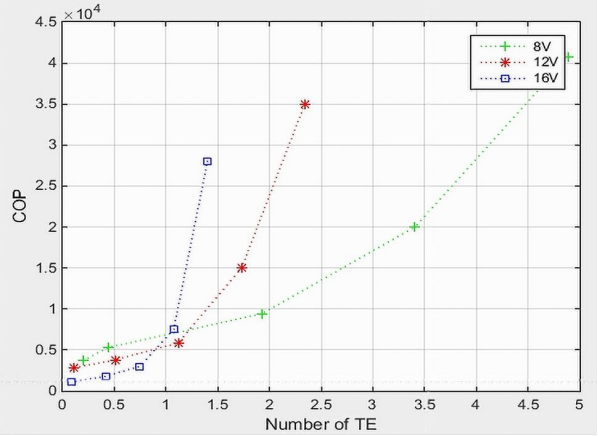

(b)

Figure 11: The relationship between COP and (a) surface temperature difference, (b) the required number of TE, for different voltages.

ing COP. In addition, the TE panel number increases as voltage increases. At a voltage of 8 V, 12 V, and 16 V the required number of TE panels is 40 000, 35 000, and 28 000, respectively.

5 Results validation

The accuracy of present theoretical results is made by the validation process. This validation presents a comparison between the results of the current theoretical study and the past theoretical study. The characters of the TE panel are chosen to validate with Akram *et al.* [17] results. Figures 12a

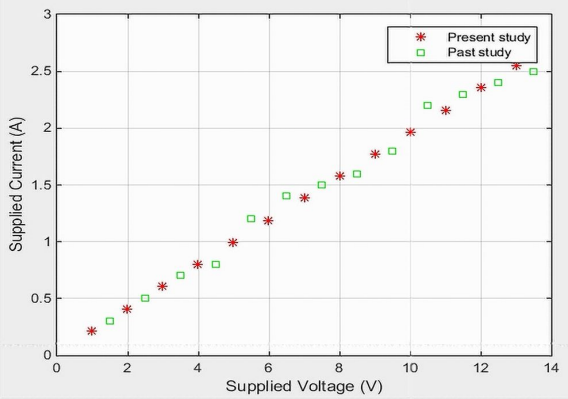

(a)

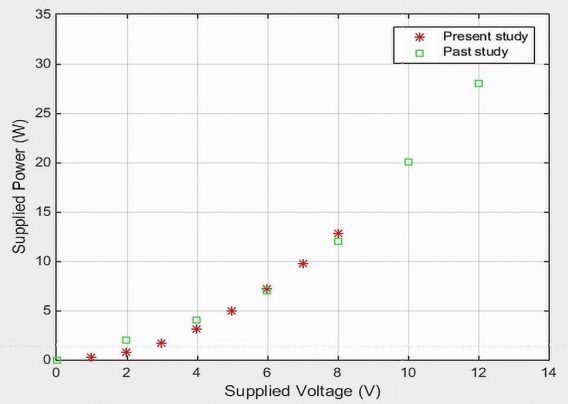

(b)

Figure 12: Comparison between present and past results: (a) supplied voltage, (b) supplied power.

and 12b present the supplied current against the supplied voltage and supplied power against supplied voltage, respectively. From the results shown it can be concluded that the same behavior between the two studies with differences in value is due to differences in input data for both studies.

6 Conclusions

In the present study, the potential of utilizing PV panels as a power source for the radiant cooling system is studied. The system consists of PV panels, controller charge, battery, TE panels, and an aluminum plate. The investigation is achieved under hot and dry weather conditions. The hourly cooling load and power consumption by TE panels for 12 months are evaluated by using the hourly analysis program, and the system design of PV panels software. The multi-paradigm programming language and numerical computing environment is used to calculate the thermal and electrical characteristics theoretically under various supplied voltages. In this study, the thermoelectric panel Joule effect is neglected to get the coefficient of performance as the reversed Carnot cycle. The results can be concluded as follows:

1. About 50% of the power consumption by TE panels is provided by PV panels.

2. The maximum power and cooling load are required by TE panels in May and June.

3. As supplied voltage increases from 1 V to 6 V, the cold surface temperature decreases from 20°C to 15°C and then increases from 15°C to 70°C as the supplied voltage increases from 6 V to 16 V.

4. As supplied voltage increases from 1 V to 16 V the hot surface temperature, surface temperature difference, supplied current, and supplied power increase from 30°C to 60°C, from 2°C to 145°C, from 1 A to 3.2 A, and from 1 W to 45 W, respectively.

5. As supplied voltage increases from 8 V to 16 V, the cooling capacity increases from 35 W to 60 W, while COP decreases from 5 to 1.5.

Received 12 June 2022

References

[1] Lyu J., Feng X., Cheng Y., Liao C.: *Experimental and numerical analysis of air temperature uniformity in occupied zone under stratum ventilation for heating mode.* J. Build. Eng. **43**(2021), 103016.

[2] Benhadid D.S., Benzaoui A.: *Refrigerants and their environmental impact. Substitution of hydro chlorofluorocarbon HCFC and HFC hydro fluorocarbon. Search for an adequate refrigerant.* Energy Proced. **18**(2012), 807–816.

[3] Witkowski A., Majkut M.: *The impact of CO_2 Compression system on the compressor power required for a pulverized coal-fired power plant in post-combustion carbon dioxide sequestration.* Arch. Mech. **59**(2012)3, 344–360.

[4] Ajirlou I.F., Kurtay C.: *Assessing the performance of the airflow window for ventilation and thermal comfort in office rooms.* Arch. Thermodyn. **42**(2021), 3, 209–242.

[5] Desmons J.: *Froid industriel: Reminder. Aide-mémoire.* Dunod, 2006 (in French).

[6] Iffa R.B., Kairouani L., Bouaziz N.: *Optimization of absorption refrigeration systems by the method of computational experiment design.* Arch. Thermodyn. **40**(2019), 1, 85–102.

[7] Ahmad S.N., Prakash O.: *Thermal performance evaluation of an earth-to-air heat exchanger for the heating mode applications using an experimental test rig.* Arch. Thermodyn **43**(2022), 1, 185–207.

[8] Najafi H., Woodbury K.A.: *Optimization of a cooling system based on Peltier effect for photovoltaic cells.* Sol. Energy **91**(2013), 152–160.

[9] Kuzichkin O.R., Konstantinov I. S., Vasilyev G.S., Surzhik D.I.: *Control of operability of Peltier modules in cooling systems based on the analysis of transient operating modes.* Arch. Thermodyn. **42**(2021), 2, 31–42.

[10] American Society of Heating, Refrigerating and Air-Conditioning Engineers. ASHRAE Handbook: Heating, Ventilating, and Air-Conditioning Systems and Equipment. ASHRAE, 2012.

[11] Xu X., Dessel V.S.: *Evaluation of prototype active building envelope window-system.* Energy Build. **40**(2008), 2, 168–174.

[12] Cheng T.C., Cheng C.H., Huang Z.Z, Liao C.G.: *Development of an energy-saving module via combination of solar cells an thermoelectric coolers for green building application.* Energy **36**(2011), 1, 133–140.

[13] Daghigh R., Khaledian Y.: *Effective design, theoretical and experimental assessment of a solar thermoelectric cooling-heating system.* Sol. Energy **162**(2018), 561–572.

[14] Irshad K., Habib K., Basrawi F., Saha B.B.: *Study of a thermoelectric air duct system assisted by photovoltaic wall for space cooling in tropical climate.* Energy **119**(2017), 504–522.

[15] PVsyst Software 7.2. https://www.pvsyst.com/download-pvsyst/ (accessed 15 March 2021).

[16] Matlab Software, 2015. https://www.mathworks.com/matlabcentral/answers/433589-how-to-download-matlab-2015a (accessed 15 March 2021).

[17] Akram M.N., Nirmani H.R., Jayasundere N.D.: *A study on thermal and electrical characteristics of thermoelectric cooler TEC1-127 series*. In: Proc. 7th Int. Conf. on Intelligent Systems, Modelling and Simulation (ISMS), 25–27 January 2016, Bangkok. IEEE 2016, 430–434.

[18] Khouri A.M., Robles M.A.O.: *Feasibility and numerical analysis of hybrid photovoltaic (pv) panels with thermoelectric cooling (TEC) systems*. In: Bringing Thermoelectricity into Reality. Intechopen, London 2018.

[19] Lim H., Jeong J.W.: *Investigation of desirable arrangement of thermoelectric modules for the radiant cooling panel*. In: 7th Int. Refrigeration and Air Condition Conf. at Purdue, 9-12 July 2018, 1928.

[20] Walikewitz N., Jänicke B., Langner M., Meier F., Endlicher W.: *The difference between the mean radiant temperature and the air temperature within indoor environments: A case study during summer conditions*. Build. Environ. **84**(2015), 151–161.

[21] Shen L., Xiao F., Chena H., Wang S.: *Investigation of a novel thermoelectric radiant air-conditioning system*. Energy Build. **59**(2012), 123–132.

[22] Seyednezhad M., Najaf H.: *Solar-powered thermoelectric-based cooling and heating system for building applications: A parametric study*. Energies **14**(2021), 5573.

[23] HAP 4.6 Software. https://www.carrier.com/commercial/en/us/software/hvac-system-design/hourly-analysis-program (accessed 15 March 2021).

[24] AutoCAD Software, 2018. https://www.freesoftwarefiles.com/3d-designing/autocad-2018-free-download (accessed 15 March 2021).